Calculation of near-edge x-ray-absorption spectra of molecules and polymers by a Green's-function method

Christoph Liegener
Institute of Physical and Theoretical Chemistry, University of Erlangen-Nürnberg, D-8520 Erlangen, Germany

Hans Ågren
Institute of Physics and Measurement Technology, University of Linköping, S-58183, Linköping, Sweden
(Received 10 December 1992)

We devise a method in which one-particle Green's-function calculations are used to obtain spectra of near-edge x-ray-absorption fine structures (NEXAFS spectra) for molecules and polymers. The x-ray rates are obtained as the residues of the retarded one-particle Green's function modulated by x-ray orbital transition moments. The spectral features are interpreted from the singularities of the spectral density of the one-particle Green's function and the site selectivity of the NEXAFS process. Utilizing this site selectivity and local-symmetry selection rules the transition moments are optionally decomposed into atomic contributions. Applications are performed for molecules in the sequence ethylene, butadiene, hexatriene, and polyacetylene. We find that the lowest bands in the discrete butadiene and hexatriene spectra are due to core excitations to the lowest π^* levels pertaining to the different core-hole sites, that the second strong-intensity regions in these spectra are composed of several strong σ excitations, and that there is a significant reduction of the π-to-σ-intensity ratio with addition of ethylene subunits. We find that the building-block principle is inappropriate; the energy and intensity features are to a large extent determined by the different relaxation responses of the creation of different core holes. Comparison with experiment, which is possible for the smaller members of the series, encourages the use of the proposed method for interpretation of polymer NEXAFS spectra.

I. INTRODUCTION

Owing to the fact that tunable synchrotron-radiation sources recently have become available in the x-ray-wavelength region there has been a resurgence of interest in x-ray-absorption spectroscopy. Modern high-resolution x-ray spectra reveal a wealth of information both in their discrete and continuum parts. This goes for spectra of free molecules as well as for solids. Recent experimental efforts have also been focused on large molecules, on model molecules of polymers, and on surface adsorbates;[1] however, there are still only few investigations directly devoted to polymers.[2–4]

Near-edge x-ray-absorption fine-structure (NEXAFS) spectroscopy essentially probes the unoccupied one-particle states of a system insofar as they are accessible by core excitation. The transitions can be further distinguished into those leading to bound states of the core excited system on the one hand, and to shape resonances in the continuum of the absorption cross section on the other hand. The former ones are visible as discrete structure in the spectra which are interpretable by either wave-function methods or propagator methods as will be discussed below, while the latter ones need a scattering theory treatment. A central concept is the so-called building-block picture, which predicts that the NEXAFS spectrum associated to a particular atom should only exhibit resonances associated with the particular type of bond of that atom. The emphasis of the present study is on the development of *ab initio* methods which are flexible enough to be applied to the bound states appearing in NEXAFS spectra of large molecular systems, in the limiting case of even polymers.

Several approaches have been reported for the calculation of NEXAFS spectra of intermediate size within the one-particle approximation. The most maintained methods are the static-exchange molecular-orbital model and the multiple scattering X_α methods. These methods cover NEXAFS spectra in both discrete and continuum parts, but interpret the NEXAFS features from quite different physical points of views: the molecular orbital and potential barrier models, respectively. Much of the applications of these models have been focused to the correlation of resonance positions with the molecular structure. For a recent review we refer the reader to Ref. 5.

Explicitly correlated methods have been used for interpreting NEXAFS spectra to a somewhat less extent. Examples are given by state specific methods, such as configuration interaction[6,7] and multiconfiguration self-consistent-field (SCF) (Ref. 8) methods, or propagator oriented methods, such as the so-called ADC-2 method.[9] Although these methods have made novel interpretations in terms of multielectron excitations[6,7] and vibronic couplings,[9] they are rather restricted to the size of the molecules that can be studied. Larger molecules have mostly been treated by multiple scattering X_α (MSX_α) and other semiempirical methods.[10] On the *ab initio* side, Green's-function or propagator methods can be advocated for large systems because of their size consistency properties.

Among such methods one possible choice could be the polarization propagator for the description of the excitation process. We want to suggest here another approach to the problem which seems promising from its conceptual and computational simplicity, and which has the advantage of taking account of correlation effects and at the same time being applicable to large systems—here, systems with periodic boundary conditions such as polymers. We apply the one-particle propagator to the core ionized system and determine its electron affinities and excitation pole strengths. The latter are modulated by molecular-orbital transition moments, which optically can be atomwise decomposed, to obtain the final NEXAFS rates. The critical approximation in the approach is the need to choose one set of orbitals and thus the neglect of orbital nonorthogonality induced by orbital relaxation between the ground and final core-excited states. We advocate here the use of an equivalent core procedure to obtain one appropriate set of orbitals pertaining to excitations from each core level. We use the sequence ethylene, butadiene, hexatriene, and polyacetylene for a demonstration. The results are compared with experiment and the performance of the model is analyzed in view of an analogous model proposed for x-ray emission.[11]

II. THEORY

As in our previous work on x-ray emission[11] we start out from the Fermi golden rule, in which the x-ray absorption rate takes the form

$$W_f \simeq E^3 |\langle \Psi_0 | \hat{T} | \Psi_f \rangle|^2 = E^3 \left| \sum_x \tau_x \chi_x \right|^2 . \tag{1}$$

In the NEXAFS case Ψ_0 and Ψ_f denote, respectively, the initial state and the core to bound excited final states of the N electron system. The rate is thus expressed as a sum of terms, each of which constitutes a product of a molecular-orbital (MO) factor τ_x and a many-body factor χ_x. The slowly varying energy factor preceding this expression is omitted for simplicity. In x-ray absorption x stands for a double index p, q, and $\hat{T}$ for the many-electron dipole operator

$$\hat{T} = \sum_{p,q} \langle \phi_p | \hat{t}_1 | \phi_q \rangle \hat{a}_p^\dagger \hat{a}_q , \tag{2}$$

where $\hat{t}_1$ is the one-electron operator, $\hat{a}_p^\dagger$, and $\hat{a}_q$ the usual creation and annihilation operators, and $\{\phi_q\}$ and $\{\phi_p\}$ sets of molecular orbitals that, in general, are mutually nonorthogonal.

Using the rules of second quantization the NEXAFS rates resolve as

$$\tau_x \chi_x = \langle \phi_q | \hat{t}_1 | \phi_p \rangle \langle \Psi_f(N) | \hat{a}_p^\dagger \hat{a}_q | \Psi_0(N) \rangle , \tag{3}$$

i.e., as a product of molecular-orbital and many-body factors. For all practical purposes, it is justified to limit the index q to one item, corresponding to the creation of a core hole at one specific site, $q=c$, due to the almost perfect orthogonality ($\chi_x \simeq 0$) between states with holes in different core orbitals or with holes in core and valence orbitals. This also complies in some sense with the fact that simultaneous two-core sited spectra are not observed. Again the same arguments as in x-ray emission apply, only that we deal with an N instead of an $N-1$ electron system and in that the core hole enters in the final instead of in the initial state. For molecules with several core-hole sites the result is a superposition of x-ray spectra (different index q) according to Eq. (3), which all can be treated separately. The molecular-orbital factor is computed here out of one set of orthogonal molecular orbitals. In the x-ray emission case it is natural to choose the set of ground-state canonical Hartree-Fock orbitals. For the NEXAFS case this set is not appropriate since the virtual orbitals are given by an N instead of an $N-1$ electron potential. We simulate here the removal of an electron from the N-electron potential by an addition of a proton, thus we optimize the set of orbitals by diagonalizing the equivalent cores $(Z+1)$ Fock matrix. For example, for ethylene the equivalent cores Fock matrix refers to $CH_2NH_2^+$. In doing so we neglect the core-virtual exchange interaction and thus singlet-triplet splitting in the NEXAFS spectrum. Since triplets are dipole forbidden, all intensity is collected into the singlets and we still obtain the correct number of states in the Green's-function calculation, although it still neglects the core-virtual exchange. The core-virtual exchange two-electron matrix elements are generally small, only a few tenths of an eV; see, e.g., work on carbonyl shake-up spectra in Ref. 12. The application of the equivalent core approximation also infers a localized broken symmetry solution for the core-excitation process.

With the three approximations outlined above, viz., truncation of the p index to one item, referring to the core orbital, the neglect of nonorthogonality (orbital relaxation), and the representation of the core-hole system by its equivalent $(Z+1)$ core, Eq. (3) is replaced by

$$\tau_x \chi_x = \langle \phi_c | \hat{t}_1 | \phi_p \rangle \langle \Psi_f(N) | \hat{a}_p^\dagger | \Psi_c(N-1) \rangle , \tag{4}$$

where

$$\Psi_c(N-1)\rangle = \hat{a}_c | \Psi_0(N) \rangle \tag{5}$$

has been introduced as a new reference state. We define a Green's function $\mathcal{G}_{kl}^c$ for this reference state:

$$\mathcal{G}_{kl}^c(\omega) = -i \int_{-\infty}^{\infty} dt\, e^{i\omega t} \langle \Psi_c(N-1) | \hat{T} \{ \hat{a}_k(t) \hat{a}_l^\dagger \} | \Psi_c(N-1) \rangle , \tag{6}$$

where $\hat{T}$ is Wick's time-ordering operator applying to $\hat{a}_k^\dagger(t)$ in the Heisenberg picture. The electronic factors in Eq. (4) are then by definition the residues of the above one-particle Green's function, Res $\mathcal{G}_{kl}^c$. Using the one-particle Green's functions the x-ray rates are therefore given as

$$W_f = \sum_{kl} \sum_{i}^{xyz} \langle \phi_l | \hat{t}_i | \phi_c \rangle \langle \phi_c | \hat{t}_i | \phi_k \rangle \mathrm{Res}_{\omega_f} \mathcal{G}_{kl}^c , \tag{7}$$

where ω_f is the pole corresponding to the final-state elec-

tron affinity of the core ionized system.

Thus under the assumptions given above the Green's-function analysis of the x-ray-absorption spectrum will be equivalent to the one for the inverse photoelectron (electron attachment) spectrum of the core-hole ion, only different molecular-orbital (MO) factors are involved. The absorbed photon's energy is related to the electron affinities EA_f^c of the core ionized system by

$$h\nu_X = IP_c - EA_f^c \ , \tag{8}$$

where IP_c denotes the core ionization potential of the neutral system. The EA_f^c values are by construction obtained as the negative of the corresponding $(N+1)$ particle poles of the above Green's function $\mathcal{G}_{kl}^c$. Only the bound-state electron affinity poles are considered in the present framework (i.e., positive EA's). We make no assumption about the initial-state ionization potentials and obtain the final x-ray energies in Eq. (8) simply by subtracting the binding energies EA_f^c from the experimental core ionization potentials. The above electron affinities are understood as $EA_f^c = E_c(N-1) - E_f(N)$ where the ground-state geometry is assumed for both states involved (vertical transitions). Since each pole corresponds to its residue entering the transition rate, the correlation properties are the same as those for the transition rates, which will be discussed below. It is interesting to observe the similarity in the treatment of x-ray absorption and emission in the present formalism. However, while the binding energies in the emission case are evidently common for different spectra pertaining to different core holes (the full spectrum is obtained from one single Green's-function calculation), they may differ in the absorption case for different core-hole sites (due to the different choices of the reference state). One thus needs one Green's-function calculation for each different core-hole site.

As for other one-particle spectra (e.g., photoelectron or x-ray emission spectra) one can distinguish the following different levels of electron correlation effects from the properties of the one-particle Green's function.

(1) $\mathrm{Res}\mathcal{G}_{kl} = \delta_{kl}\delta_{kq}$ for a particular q. The Hartree-Fock picture is retained which implies that the energetics of the x-ray spectrum can be analyzed by Koopmans theorem, and intensities by the MO factor τ_q alone. This in turn can be conducted in terms of MO theory, local densities, and effective and strict selection rules as further demonstrated below.

(2) $\mathrm{Res}\mathcal{G}_{qq}$ is close to 1 for a particular q. The quasi-particle picture holes. An MO analysis is still possible.

(3) More than one $\mathcal{G}_{qq}$ enters in the residues. This leads to particle-mixing (hole-mixing) effects, and electronic interference in transition cross sections.

(4) No single $\mathcal{G}_{qq}$ has a large contribution to the residues. One can then not associate a 1-1 correspondence between MO's [or MO factors in Eq. (1)] and spectral bands (states). The states in question are thus associated with a breakdown of the molecular-orbital picture.

While this type of analysis is common for valence photoionization it is more rare concerning x-ray spectra for which, to our knowledge, it has been applied only in the emission case.[6,11] It should be pointed out that the conditions are not the same for the generation of particle mixing in x-ray absorption (or breakdown effects) as for hole mixing in photoemission. Inner hole states can couple through near-degenerate semi-internal hole-particle excitations. This particular type of coupling has no counterpart in the NEXAFS case. This is because only the first electron affinities of the ion lead to bound states. They show a similar behavior as the occupied outer valence orbitals in the photoionization or x-ray emission cases, which seldom undergo breakdown effects. On the other hand, breakdown effects appearing as channel mixing can be expected to further complicate the situation for shape resonances in the continuum. This is, however, not considered here.

The analysis of NEXAFS spectra can be further simplified by decomposing the molecular-orbital factor τ_q by expanding the MO's $\{\phi\}$ in a linear combination of atomic orbitals (LCAO) $\{\chi\}$; $\phi_k = \sum_\nu c_\nu^k \chi_\nu$ in the spirit of the intensity model for molecular x-ray emission.[13] The transition rates are then expressed in the following way:

$$W_f = \sum_{i,\mu,\nu} M_{c\mu}^i M_{c\nu}^{i*} \sum_{kl} c_{\mu l} c_{\nu l}^* \mathrm{Res}_{\omega_f} \mathcal{G}_{kl} \tag{9}$$

where $M_{c\mu}^i = \langle \phi_c | \hat{r}_i | \phi_\mu \rangle$ are the dipole matrix elements between the core hole ϕ_c and the μth atomic orbital. The x, y, or z components of the dipole transition operator are explicitly introduced here by index i. We will restrict ourselves here to transitions near the K edge of first row compounds. This means that c is a $1s$ hole at a given atom A. We neglect terms in Eq. (9) that correspond to cross transitions from atom A to any other atom (the so-called one-center approximation). Since χ_c is a $1s$ orbital and selection rules in $M_{i\mu}$ require that μ must be a $2p$ orbital, Eq. (9) simplifies to

$$W_f = |M_{1s,2p}|^2 \sum_{kl} \left[\sum_{\mu \in 2p_A}^{x,y,z} c_{\mu k} c_{\mu l}^* \right] \mathrm{Res}_{\omega_f} \mathcal{G}_{kl} \tag{10}$$

if the above LCAO expansion involves only a single-zeta (SZ) basis set. Here $|M_{1s,2p}|^2$ is a common factor that can be neglected for relative intensities. If an n-zeta basis set is used (double-zeta, triple-zeta, etc., with or without d functions), then Eq. (10) reads as

$$W_f = \sum_{st}^{1,n} M_{cs} M_{ct}^* \sum_{kl} \left[\sum_{\mu \in 2p_A}^{x,y,z} c_{s\mu k} c_{t\mu l} \right] \mathrm{Res}_{\omega_f} \mathcal{G}_{kl} \ , \tag{11}$$

where s,t are indices of expansion of MO ϕ_k over the atomic orbitals χ_μ of a particular symmetry ($2p$ for the first row case) and center. In this case only the radial integrals M_{cs} need to be considered. Other types of transitions (near the L or M edges of heavier elements) can be treated in an analogous way, only different radial integrals with different angular coefficients appear. Corresponding equations have been derived in the context of x-ray emission spectra.[11]

For the polymer case we use a Koster-Slater-type method.[14,15] We based our perturbation treatment on *ab initio* calculations with correlation of the bulk as well as of the clusters (with and without perturbation). While it

is impractical to explicitly iterate for effects of the local perturbation on self-consistency[16–19] if one is interested only in the bound states, we obtain a parameter-free (non-tight-binding) description of the emergence of bound states under influence of the perturbation. We like to mention that the system investigated here, polyacetylene, has been treated by related methods in the context of other local effects than those occurring here; in particular, polaron-type defects.[20,21] We use the method to calculate the bound states induced in the band gap of polyacetylene by the presence of the defect representing the equivalent core for the $C1s$ hole. This means we have to solve the equation

$$\det[1-\tilde{\mathcal{G}}^0(\omega)V(\omega)]=0\ , \tag{12}$$

where $\tilde{\mathcal{G}}^0$ is the (correlated) one-particle Green's function of the periodic system in the contravariant atomic orbital basis:

$$\tilde{\mathcal{G}}^0(\omega)_{\mu H,\nu J}=\frac{1}{2\pi}\sum_l \int_{-\pi}^{\pi} dk\ c_{\mu l}(k)c^*_{\nu l}(k) \times\frac{P_l(k)e^{ik(R_H-R_J)}}{\omega-\omega_l(k)}\ , \tag{13}$$

where μ,ν are atomic orbital and H,J cell indices, $\omega_l(k)$ and $P_l(k)$ are the quasiparticle bands and the corresponding residues of the one-particle Green's function of the periodic system, and $c_{\mu l}$ are the Hartree-Fock crystal orbital eigenvector coefficients. The defect matrix of the inverse one-particle Green's function is given by

$$V_{\mu,\nu}=\sum_l c^p_{\mu l}c^{p*}_{\nu l}\frac{\omega-\omega^p_l}{P^p_l}-\sum_l c^0_{\mu l}c^{0*}_{\nu l}\frac{\omega-\omega^0_l}{P^0_l}\ , \tag{14}$$

where $c^0_{\mu l}$, and $c^p_{\mu l}$ are the cluster Hartree-Fock eigenvector coefficients for the unperturbed and the equivalent core system, respectively, and ω^0_l and P^0_l are the corresponding poles and residues of the cluster one-particle Green's functions, respectively. The dimension of the above secular problem is determined by the cluster size inherent in the atomic orbital indices of V; it comprises six CH_2 units in a double-zeta basis in our case. The transition rates are obtained as above, but using the eigenvector components of the Koster-Slater matrix.

III. COMPUTATIONAL DETAILS

Calculations have been carried out for several basis sets: single zeta (Tatewaki and Huzinaga[22]) and double zeta including or excluding polarization functions (Gianolio and Clementi[23]). The one-particle Green's-function calculations were all performed with the second-order irreducible self-energy part. The molecular-orbital factors were evaluated from canonical Hartree-Fock orbitals for the equivalent core states, employing the length form of the transition dipole operator. The Hartree-Fock calculations on the periodic system were performed by the *ab initio* crystal orbital method[24–26] using 801 k points, the strict 9th neighbors' interaction approximation and a double-zeta basis set at Suhai's geometry.[27] The procedure to obtain the quasiparticle shifts has been the same as described before,[28,29] namely, for 9 k points and invoking the second neighbors' interaction approximation and interpolating to 801 k points by spline interpolation. The virtual excitation space was exhausted for all except the core orbitals and their virtual images. All k integrations were performed by the summed Simpson rule for 801 points in the irreducible part of the Brillouin zone. The results are given in Table I–III and compared to experimental spectra in Figs. 1–3.

TABLE I. Ethylene Green's function results (main poles) for bound-state electron affinities of core ionized system. The asterisk signifies that the experimental core IP is used to obtain the kinetic energy: $I=290.88$ eV (from Ref. 32).

No.	Symmetry	Orbital Energy	Pole	Strength	Rate * 100	E^*_{kin}
a						
1	Π	−7.83	−8.40	0.934	0.172	282.48
2	Σ	−0.64	−1.51	0.952	0.047	289.37
3	Σ	0.38	−0.44	0.956	0.310	290.44
b						
1	Π	−4.73	−5.46	0.924	0.259	285.42
2	Σ	−2.45	−2.94	0.974	0.030	287.94
3	Σ	−1.30	−1.79	0.975	0.148	289.09
4	Σ	−1.23	−1.63	0.980	0.003	289.25
c						
1	Π	−4.30	−5.66	0.918	0.247	285.22
2	Σ	−2.48	−3.13	0.973	0.031	287.75
3	Σ	−1.18	−1.70	0.979	0.002	289.18
4	Σ	−1.17	−1.83	0.973	0.144	289.05

[a]Single-zeta second order.
[b]Double-zeta second order.
[c]Double-zeta polarization, second order.

TABLE II. Butadiene Green's-function that results (main poles) for bound-state electron affinities of core ionization system. The asterisk signifies the experimental core IP's are used to obtain kinetic energy: I(middle)=290.81 eV, I(end)=289.21 eV (from Ref. 32).

No.	Symmetry	Orbital Energy	Pole	Strength	Rate * 100	E^*_{kin}
a						
1	Π	−7.32	−8.05	0.902	0.143	282.76
2	Π	−2.02	−2.51	0.882	0.054	288.30
3	Σ	0.06	−1.03	0.940	0.164	289.78
b						
1	Π	−7.30	−7.93	0.909	0.102	282.28
2	Π	−1.49	−2.93	0.856	0.025	287.28
3	Σ	0.02	−1.06	0.930	0.051	289.15
c						
1	Π	−4.63	−5.59	0.896	0.206	285.22
2	Σ	−1.81	−2.49	0.965	0.082	288.32
3	Σ	−0.90	−1.53	0.965	0.004	289.28
4	Σ	−0.02	−0.62	0.968	0.003	290.19
5	Π	0.03	−1.14	0.884	0.108	289.67
d						
1	Π	−4.51	−5.27	0.901	0.097	284.94
2	Σ	−1.48	−2.21	0.957	0.017	288.00
3	Σ	−0.81	−1.46	0.968	0.023	288.75
4	Σ	−0.18	−0.81	0.967	0.019	289.40
5	Π	0.83	−0.97	0.874	0.029	289.24

[a]Single-zeta second order, middle carbon 1s.
[b]Single-zeta second order, end carbon 1s.
[c]Double-zeta second order, middle carbon 1s.
[d]Double-zeta second order, end carbon 1s.

IV. RESULTS

The NEXAFS spectra of the three oligomer molecules addressed here—ethylene, butadiene, and hexatriene—have been studied rather extensively by synchrotron x-ray-absorption spectroscopy. For some recent high-resolution studies we refer the reader to Refs. 9, 30 (ethylene) and 8 (butadiene and hexatriene).

A. Ethylene

The ethylene molecule has been studied on several occasions in both free and chemisorbed forms[30,1]. The high-resolution spectra show three bands with rather anomalous internal fine structures. For the $C1s$-π^* band this structure has been interpreted in terms of vibronic coupling mechanisms.[9] Our calculated energies and intensities for the first three dipole-allowed transitions to the $1b_{2g}$, $4a_g$, and $2b_{2u}$ levels reproduce those of the experimental spectrum quite well; the intensity for the second transition is somewhat too low (see Fig. 1).

B. Butadiene

As seen in Fig. 2 the low-energy part of the butadiene spectrum contains an intensive double-band feature. This feature is well reproduced by the Green's-function calculation. The results essentially agree with previous ΔMCSCF (multiconfiguration SCF) calculations[8] although with better relative intensities and absolute excitation energies. The present calculation thus confirms the interpretation[8] of this double-peak feature as due to chemically shifted transitions to the first π^* level from the end and mid carbons; other, evidently incorrect, interpretations have been given earlier (see discussion in Ref. 8). Further up in the butadiene spectrum, at 287–289 eV, there is an odd three peak structure, and even higher up one finds broad features ranging between 10 and 30 eV above the ionization threshold, assigned to σ(C—C) and σ(C=C) type shape resonances.[31] The interpretation of the 287–289 feature is controversial. Three peaks were indeed predicted by the MCSCF calculations in Ref. 8, but with small intensities and somewhat displaced energies. A statement was therefore made that σ-type excitations contribute to this feature (ΔMCSCF utilized a small complete active Π space-type wave function, thereby excluding excitations among the Σ manifold of orbitals). However, this contradicted the findings from measurements of butadiene on a surface [butadiene monolayer on Ag(110)] by Coulman *et al.*[31] In that work the existence of a second π^* level at 288 eV was derived from the polarization dependency. At grazing x-ray incidence this band and the first (there unresolved) π^* band at 285 eV dominated, while these bands nearly vanished at normal x-ray incidence. The polarization dependence of the three higher lying resonances, assigned as C—H*, σ^*_{C-C}, and $\sigma^*_{C=C}$ was reversed, the C—H* structure was, however, not separated from the "second π^*" structure. This was shown as an example of where the orientation of a molecule on a surface and the symmetry selection rules can be used to assign a new spectral feature. It is therefore interesting that the Green's-

function calculations predict a number of peaks in the region, the two lower, more intensive, ones are of σ symmetry the higher one of π symmetry, see Table II. The large intensity indicates by itself the valence character of these excitations. We feel that a higher resolved spectrum of butadiene oriented by physisorption (instead of by chemisorption) would be helpful to resolve this apparent contradiction. In any case, the present and past[8] calculations reject the notation of two single π^* levels at 284 and 288 eV as inferred from a building-block principle (see further discussion below).

C. Hexatriene

The hexatriene spectrum shows two broad, about equally intense bands. We see from Table III that the first band should be assigned as due to the three $C1s$-π^* transitions, with the end carbon having the lowest excitation energy and the middle carbon the highest. It can be noted that the end carbon also has the lowest ionization potential (IP) but that the middle carbon has the highest.[32] Since initial state effects are ignorable for core IP's of hydrocarbons, this reflects differences in the core-hole screening relaxation between the ionization and excitation cases. A high-resolution recording in Ref. 8 clearly showed fine structure for the first band, which must be interpreted as due to vibrational effects. The second main band is composed of some six transitions gathered into a narrow interval.

D. Polyacetylene

When applying the Koster-Slater formalism to the core ionized system as suggested above, we make the surpris-

TABLE III. Hexatriene Green's-function results (main poles) for bound-state electron affinities of core ionization system. The asterisk signifies that the experimental core IP's are used to obtain kinetic energy: I(middle)=290.23 eV, I(next)=290.56 eV, I(end)=289.82 eV (from Ref. 32).

No.	Symmetry	Orbital Energy	Pole	Strength	Rate * 100	E^*_{kin}
a						
1	Π	−7.03	−7.79	0.895	0.096	282.44
2	Π	−1.69	−2.53	0.872	0.004	287.70
3	Π	−0.78	−2.14	0.854	0.065	290.11
4	Σ	1.24	−0.12	0.924	0.198	288.09
b						
1	Π	−6.98	−7.82	0.880	0.133	282.74
2	Π	−2.98	−3.60	0.865	0.054	286.96
3	Σ	0.49	−0.76	0.931	0.183	289.80
4	Π	1.36	−0.11	0.850	0.001	290.45
5	Σ	2.33	−0.10	0.888	0.099	290.46
c						
1	Π	−6.90	−7.60	0.893	0.076	282.22
2	Π	−2.32	−3.60	0.848	0.138	286.22
3	Σ	0.94	−0.34	0.917	0.044	289.48
4	Π	1.01	−0.98	0.833	0.005	288.84
d						
1	Π	−4.52	−5.55	0.889	0.142	284.68
2	Σ	−1.02	−1.84	0.956	0.072	288.39
3	Σ	−0.31	−1.02	0.961	0.016	289.21
4	Π	0.25	−1.06	0.881	0.015	289.17
5	Σ	0.26	−0.43	0.961	0.004	289.80
e						
1	Π	−4.35	−5.38	0.881	0.182	285.18
2	Σ	−1.51	−2.24	0.959	0.078	288.32
3	Π	−0.86	−2.03	0.870	0.110	288.53
4	Σ	−0.61	−1.32	0.956	0.005	289.24
5	Σ	0.53	−0.18	0.957	0.005	290.38
f						
1	Π	−4.26	−5.16	0.888	0.106	284.66
2	Σ	−0.90	−1.75	0.949	0.014	288.07
3	Σ	−0.43	−1.16	0.961	0.020	288.66
4	Π	−0.02	−1.63	0.863	0.101	288.19
5	Σ	0.57	−0.13	0.960	0.001	289.69

[a]Single-zeta second order, middle carbon 1s.
[b]Single-zeta second order, next carbon 1s.
[c]Single-zeta second order, end carbon 1s.
[d]Double-zeta second order, middle carbon 1s.
[e]Double-zeta second order, next carbon 1s.
[f]Double-zeta second order, end carbon 1s.

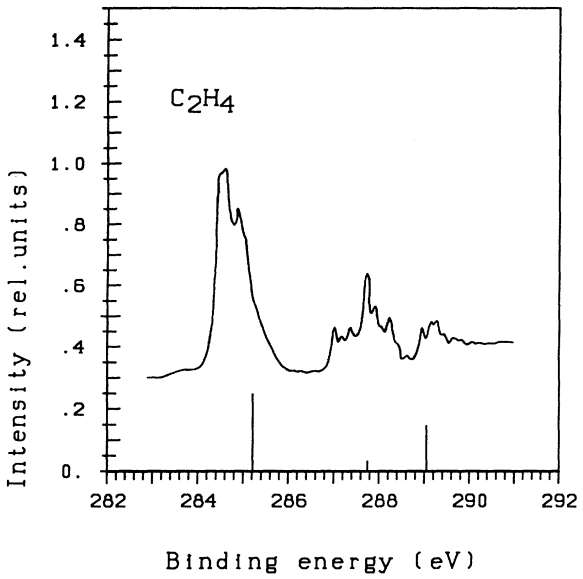

FIG. 1. Comparison of the calculated x-ray-absorption spectrum of ethylene with the experimental spectrum of Ref. 9.

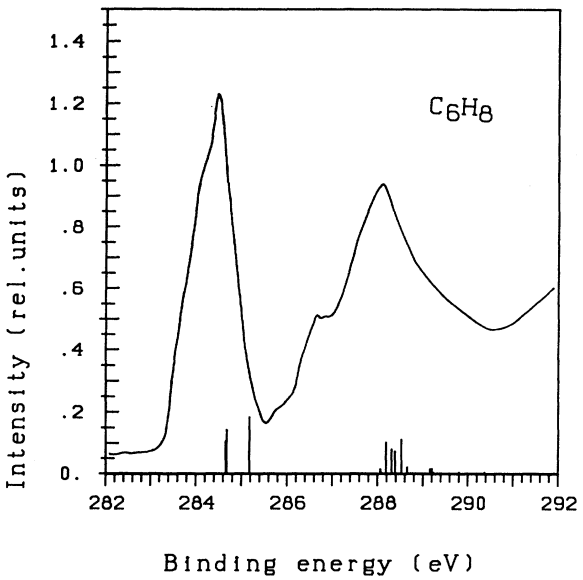

FIG. 3. Comparison of the calculated x-ray-absorption spectrum of hexatriene with the experimental spectrum of Ref. 8.

ing observation that for π symmetry the bound-state electron affinity of the core ionized system falls into the valence band region of the unperturbed system. The bound state formalism does then no longer apply for this state and we have to place its affinity at the top of the valence band. The theoretical value for this is -5.32 eV, the experimental value of Salaneck *et al.*[33] is -4.5 eV. The uncorrelated calculation places the π electron affinity pole of the core ionized polymer at -4.84 eV, the transition rate is less than 1% of that of the oligomers. The vanishing of the transition rate for this state indicates delocalization of the screening π electrons, in agreement with the above finding that those states seem to interact strongly with the bulk plane-wave states. This trend is already indicated by the oligomer results (see Table IV), where the lowest π state transition rates for a middle $C1s$ hole are rapidly decreasing with chain length. On the other hand, the energetic position of the $C1s$-π^* absorption seems not to change dramatically from the oligomers to the polymer, an observation consistent with an estimated $C1s$ IP of 290.2 eV (Ref. 32) for the polymer.

A different behavior than for the π states is displayed by the σ-type bound states. For these states the transition rates remain of the same order of magnitude for all chain lengths, which indicates less delocalized states. The binding energy with respect to the core IP is becoming slightly smaller for the polymer than for the oligomers. The electron affinity of the core ionized system is situated well inside the fundamental gap, almost 1 eV below the lower conduction band edge, the theoretical value of which is -0.80 eV.

The experimental core excitation spectrum of Ritsko[2]

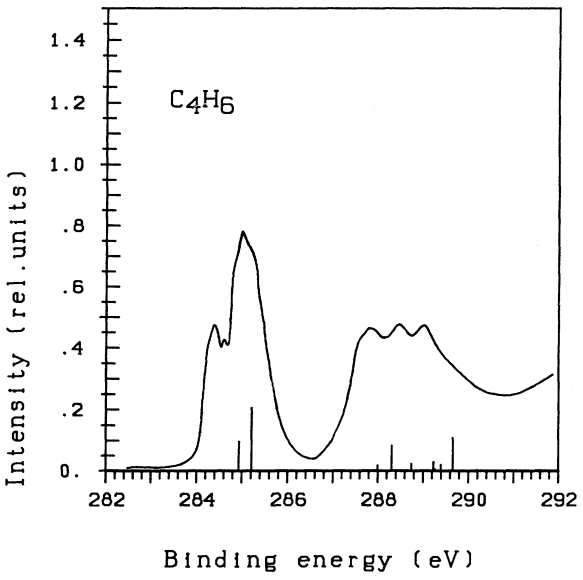

FIG. 2. Comparison of the calculated x-ray-absorption spectrum of butadiene with the experimental spectrum of Ref. 8.

TABLE IV. Polyacetylene Green's-function results for bound-state electron affinities of core ionized system in comparison to oligomer results. Energies in eV, rates in 100 au.

	C_2H_4	C_4H_6	C_6H_8	$(C_2H_2)_x$	$(C_2H_2)_x^a$
b					
Pole	-5.46	-5.59	-5.55	$(-5.32)^c$	-4.84
Rate	0.249	0.206	0.142		0.001
d					
Pole	-2.94	-2.49	-1.84	-1.60	-1.22
Rate	0.030	0.082	0.072	0.047	0.066

[a]Uncorrelated results.
[b]Bound state of Π symmetry.
[c]Upper valence band edge (theoretical).
[d]Bound state of Σ symmetry.

has a peak at 284.1 eV which should be a π state. Comparison with our results would, however, not be conclusive because the electron transmission method employed for that experiment does not exclude additional peaks due to smaller fragments occurring after radiation damage, as has been evidenced in the case of polyethylene before.[34] The interesting question of how far the intensity of the π band is reduced with respect to the intensity of the σ band thus remains open, also because the experimental spectrum displays only this (π) band in the energy range studied.

V. DISCUSSION

Using a one-particle interpretation of NEXAFS, there is a one-to-one correspondence between spectral features and molecular orbitals. An examination of the NEXAFS intensities can be obtained by analyzing the "improved virtual orbitals" given as canonical orbitals from the equivalent cores Fock operator, as here, or alternatively by a static exchange type calculation. The one-center decomposition of these orbitals leads to an intensity analysis for NEXAFS given by Eq. (11). In the x-ray emission case a critical examination of this decomposition has been given in Refs. 35 and 36. For NEXAFS spectra of first row species this means that states referring to valence like $2p$-containing π^* orbitals receive considerable intensity. The amount of intensity depends evidently on the degree of localization to the site of the created core hole. In π conjugated systems one can expect a complete screening of the core hole by the "π electron," meaning that each such NEXAFS state should receive large intensity. These states will still be chemically shifted, because the screening hole will be differently distributed for different core excitations, as is verified for butadiene in Refs. 8 and 32. It is interesting to note from Table II, also confirmed by MCSCF calculations in Ref. 8, that the lowest π^* level receives large x-ray rates for the two core sites in butadiene, while the second π^* level in each case gets lower rates. We interpret this as due to different screening and localization properties of the two levels, in particular the second π^* level electrons do not participate in the core screening to the same extent as first π^* level electrons do for the lower excitations, but remain more delocalized. Thus in a one-particle picture we expect the number of intense π^* excitations simply to equal the number of chemically different core sites.

The analysis of experiments quoted in Refs. 37 and 38 were conducted by means of MO theory. Such a proceeding is supported by examination of the pole strengths in Table II. Taking butadiene as an example, the 10 pole strengths listed, both middle-atom and end-atom included, ranges between 0.87 and 0.97, and are thus both large and relatively little varying. In the terminology of photoemission we can therefore state that the quasiparticle picture holds, which, according to item (2) in Sec. II, entails an MO analysis in terms of the equivalent core orbitals as well as the atomic decomposition model. In Ref. 8 a rather considerable configuration mixing was observed for some of the states, however, the two approaches are not directly comparable, since in MCSCF the set of orbitals are reoptimized (simultaneously with the configurational coefficients) for each state, while in the Green's-function approach a common set is used for all states pertaining to a given core level. Even if MO theory is applicable, orbital energies might be of insufficient accuracy to order the transitions correctly since splittings of states become small for the larger species and at higher excitation energies. The Green's-function results also allocate more states with negative electron affinities than what is derived from orbital eigenvalues. Surprisingly large changes occur when going from minimal to double-zeta basis sets for ethylene. On the other hand, the change upon inclusion of polarization functions is perhaps smaller than could be expected. We therefore decided to use the double-zeta basis set for the more extended systems. Here, this has also allowed us to combine the Koster-Slater method with correlated one-particle Green's-function results for the periodic system which were previously obtained with the same basis set [28] and which were important in the context of interpreting photoelectron spectra.[39]

Our interpretations, being quite different from the standard ones, take into account the effect of relaxation, which is known to have an important bearing on the analysis of a number of different core electron spectroscopies. The standard interpretation of the butadiene spectrum is based on the fact that conjugation leads to two split antibonding π^* orbitals.[1] According to the building-block principle the excitations should energy- and intensity-wise be close to that of ethylene; two π^* excitations occur because of the interaction and splitting of the two $C{=}C$ π^* orbitals when two ethylene molecules form butadiene. In the present interpretation, however, we note that the splitting is largely caused by a shift, a final-state relaxation shift, due to the screening of the two core holes. Because the chemical environment is different this relaxation is quite different, in particular, end atoms are less relaxed than mid atoms, because of fewer polarization centers within a given radius. This difference in relaxation leads to large differences in transition moments, in butadiene it led to a two state appearance because the second π^* level is weaker for both the end- and the mid-atom excitations. Likewise for hexatriene the three-state appearance (two are quasidegenerate) is due to different relaxation of the three core-hole wave functions, and not due to the presence of three ethylene building blocks.

In analogy with the x-ray emission case[11] we take interest in how the orbital localization that fingerprints the spectrum of the small subunit is gradually distorted in the process of delocalization. In general, while the polymer (here polyacetylene) and the smallest subunit (here ethylene) contains only identical carbon atoms, all other members of the oligomer sequence contain unequal carbon atoms, inducing different relaxation induced shifts. This leads to initial state chemical shifts that displace the accompanying NEXAFS transitions leading to a total spectrum of several overlapping core-sited subspectra. A recent study of the core electron chemical shifts[32] shows that there is a regular attentuating trend of end to bulk atom binding energies converging to the polyacetylene

value, thereby displaying a quasi one-dimensional analogue of surface to bulk chemical shifts. The effect of this on the x-ray emission spectrum[11] is a gradual overall broadening going from ethylene to hexatriene, which turns into a sharpening as the "bulk" atoms with small shifts outnumber the end atoms with larger shifts. The same trend is obtained in the corresponding NEXAFS spectra.

VI. CONCLUSIONS

We have presented a method in which one-particle Green's-function calculations are used to obtain spectra of near-edge x-ray-absorption fine structures (NEXAFS spectra) for molecules and polymers. The x-ray rates are obtained as the residues of the retarded one-particle Green's function modulated by x-ray orbital transition moments. Applications are performed for molecules in the sequence ethylene, butadiene, hexatriene, and polyacetylene. We find that the lowest bands in the discrete butadiene and hexatriene spectra are due to core excitations to the lowest π^* levels pertaining to the different core-hole sites, which is in line with earlier MCSCF predictions.[8] The two-peak feature in butadiene is thus due to different relaxation mechanisms for the two (end and middle) core-sited states. This relaxation gives rise to a shift for the lowest π^* levels and a considerable reduction of the transition moments to the second π^* level.

Calculations indicate a somewhat smaller role of multielectron effects than predicted by MCSCF calculations.[8] The one-particle approximation is sufficiently well recovered by the Green's-function calculations to warrant an MO analysis. However, the molecular orbitals to be used for interpretation should be the ones corresponding to the final states, relaxed and relocalized according to each particular core hole. The building-block picture in which the larger oligomer spectra are derived from overlapping orbitals of the ethylene subunits is not warranted. The calculations predict that the onset of discrete σ-type transitions occurs at a lower energy than predicted from experiments with surface-adsorbed butadiene.[31] Our calculations established a reduction in the π:σ intensity ratio going along the oligomer sequence. This trend can also be traced for the polymer, where our calculations show that a significant reduction of the π:σ intensity ratio might be expected for polyacetylene NEXAFS compared to the oligomer spectra.

We have presented working expressions for intensity analysis based on an atomic decomposition of orbitals, both in the oligomer and polymer cases. In the spirit of the one-center model for x-ray emission[13] given for polymers in Ref. 11, these expressions can be used for a simplified analysis of NEXAFS spectra. The findings stated above that the NEXAFS spectra are much dependent on the particular relaxation of each core hole indicate that the one-center analysis should be performed separately for each such case. The use of a common set of orbitals as in the emission case (often the canonical ground-state Hartee-Fock orbitals) thus seems to be less warranted in the NEXAFS case. Other approximations, like neglect of two-center contributions and nonorthogonality, are probably of equal quality in the absorption and emission cases. To establish this conclusively would require further detailed analyses covering a set of different molecules.

ACKNOWLEDGMENTS

We acknowledge valuable discussions on NEXAFS spectroscopy with Anders Nilsson and Nils Mårtensson. This work was supported by a grant from CRAY Research Inc.

[1]J. Stöhr, *NEXAFS Spectroscopy* (Springer, Berlin, 1992).
[2]J. J. Ritsko, Phys. Rev. Lett. **46**, 849 (1981).
[3]J. Stöhr, D. A. Outka, K. Baberschke, D. Arvantis, and J. A. Horsley, Phys. Rev. B **36**, 2976 (1987).
[4]T. Ohta, K. Seki, T. Yokomaya, I. Morisada, and K. Edamatsu, Phys. Rev. Lett. **46**, 849 (1981).
[5]J. A. Sheehy, T. J. Gil, C. L. Winstead, R. E. Farren, and P. W. Langhoff, J. Chem. Phys. **91**, 1796 (1989).
[6]H. Ågren and R. Arneberg, Phys. Scr. **28**, 80 (1983).
[7]H. Ågren, R. Arneberg, J. Müller, and R. Manne, Chem. Phys. **83**, 53 (1984).
[8]A. Naves de Brito, S. Svensson, N. Correia, M. P. Keane, H. Ågren, O. P. Sarinen, A. Kivimäki, and S. Aksela, J. Electron Spectrosc. Relat. Phenom. **59**, 293 (1992).
[9]F. X. Gadea, H. Köppel, J. Schirmer, L. S. Cederbaum, K. J. Randall, A. M. Bradshaw, Y. Ma, F. Sette, and C. T. Chen, Phys. Rev. Lett. **66**, 883 (1991).
[10]A. P. Hitchcock, in *Collision Processes of Ion, Positron, Electron and Photon Beams with Matter,* Proceedings of Escola Latino-America de Fisica ELAF-91 (4–24 Au. 1991) (World Scientific, Singapore, 1991).
[11]C.-M. Liegener and H. Ågren (unpublished).
[12]D. Nordfors, A. Nilsson, N. Mårtensson, S. Svensson, U. Gelius, and H. Ågren, J. Electron Spectrosc. Relat. Phenom. **56**, 117 (1991).
[13]R. Manne, J. Chem. Phys. **52**, 5733 (1970).
[14]G. F. Koster and J. C. Slater, Phys. Rev. **96**, 1208 (1954).
[15]J. Callaway, Phys. Rev. B **3**, 2556 (1971).
[16]J. Ladik and M. Seel, Phys. Rev. B **13**, 5338 (1976).
[17]J. Ladik, Phys. Rev. B **17**, 1663 (1978).
[18]G. Baraff and M. Schlüter, Phys. Rev. B **19**, 4965 (1979).
[19]J. Bernholc, N. O. Lipari, and S. T. Pantelides, Phys. Rev. B **21**, 3545 (1980).
[20]M. Seel, Solid State Commun. **52**, 467 (1984).
[21]M. Boman and S. Stafström, Synth. Metals, Proc. ICSM'1992 (to be published).
[22]H. Tatewaki and S. Huzinaga, J. Comp. Chem. **1**, 205 (1980).
[23]L. Gianolio and E. Clementi, Gazz. Chem. Ital. **110**, 179 (1980).
[24]G. Del Re, J. Ladik, and G. Biczo', Phys. Rev. **155**, 337 (1967).
[25]J. M. Andre', L. Gouverneur, and G. Leroy, Int. J. Quant. Chem. **1**, 427 (1967).
[26]J. M. Andre', L. Gouverneur, and G. Leroy, Int. J. Quant.

Chem. **1**, 451 (1967).
[27]S. Suhai, Phys. Rev. B **27**, 3506 (1983).
[28]C.-M. Liegener, Chem. Phys. Lett. **167**, 555 (1990).
[29]C.-M. Liegener, A. Naves de Brito, H. Ågren, W. J. Griffiths, and S. Svensson, Phys. Rev. B **46**, 11 295 (1992).
[30]D. Arvantis, J. Singh, H. Rabus, T. Ledere, and K. Baberschke, Phys. Rev. B **45**, 1518 (1991).
[31]D. Coulman, J. L. Solomon, R. J. Madix, and J. Stöhr, Surf. Sci. **257**, 97 (1991).
[32]A. Naves de Brito, S. Svensson, M. P. Keane, L. Karlsson, H. Ågren, and N. Correia, Europhys. Lett. **20**, 205 (1992).
[33]W. R. Salaneck, H. R. Thomas, C. B. Duke, A. Paton, E. W. Plummer, A. J. Heeger, and A. G. MacDiamid, J. Chem. Phys. **71**, 2044 (1979).
[34]J. J. Ritsko, J. Chem. Phys. **70**, 5343 (1979).
[35]H. Ågren and J. Nordgren, Theor. Chim. Acta **58**, 111 (1981).
[36]H. Ågren and A. Flores-Riveros, J. Electron Spectrosc. Relat. Phenom. **56**, 259 (1991).
[37]A. P. Hitchcock, S. Beaulieu, T. Steel, J. Stöhr, and F. Sette, J. Chem. Phys. **80**, 3927 (1984).
[38]R. N. S. Sodhi and C. E. Brion, J. Electron Spectrosc. Relat. Phenom. **37**, 1 (1985).
[39]C.-M. Liegener, Phys. Rev. **47**, 1607 (1993).